# Structural and Functional Effects of Multiple Mutations at Distal Sites in Cytochrome *c*[†,‡]

Terence P. Lo,[§] Sonja Komar-Panicucci,[||] Fred Sherman,[⊥] George McLendon,[||] and Gary D. Brayer*[,§]

*Department of Biochemistry, University of British Columbia, Vancouver, British Columbia, Canada V6T 1Z3, and Departments of Chemistry, Biochemistry, and Biophysics, University of Rochester, Rochester, New York, 14642*

*Received September 28, 1994; Revised Manuscript Received January 9, 1995*[⊗]

ABSTRACT: Multiple mutations at distally located sites have been introduced into yeast iso-1 cytochrome *c* to determine the contributions of three amino acids to the structural and functional properties of this protein. The mutant proteins, for which high-resolution structures were determined, included all possible combinations of the substitutions Arg38Ala, Asn52Ile, and Phe82Ser. Arg38, Asn52, and Phe82 are all conserved in the primary sequences of eukaryotic cytochromes *c* and have been shown to significantly affect several properties of these proteins including protein stability, heme reduction potential, and oxidation state dependent conformational changes. The present studies show that the structural consequences of each amino acid substitution in combinatorial mutant proteins were similar to those observed in the related single-mutant proteins, and therefore no synergistic effect between mutation sites was observed for this feature. With respect to protein stability, the effect of individual mutations can be understood from the structural changes observed for each. It is found that stability effects of the three mutation sites are independent and cumulative in multiple-mutant proteins. This reflects the independent nature of the structural changes induced at the three distally located mutation sites. In terms of heme reduction potential two effects are observed. For substitution of Phe82 by serine, the mechanism by which reduction potential is lowered is different from that occurring at either the Arg38 or the Asn52 site and is independent of residue replacements at these latter two positions. For Arg38 and Asn52, overlapping interactions lead to a higher reduction potential than expected from a strict additive effect of substitutions at these residues. This appears to arise from interaction of these two amino acids with a common heme element, namely, the heme propionate A group. The present results underscore the difficulty of predicting synergistic effects of multiple mutations within a protein.

Cytochrome *c* functions as the penultimate electron acceptor in the mitochondrial electron transport chain (Moore & Pettigrew, 1990). A focus of protein engineering studies designed to elucidate the structural and functional basis of electron transfer mediated by this protein has been yeast iso-1 cytochrome *c*, the structure of which has been studied to high resolution in both the reduced and oxidized states (Louie & Brayer, 1990; Berghuis & Brayer, 1992). In particular, studies of specifically constructed mutants of yeast iso-1 cytochrome *c* have been carried out to determine the roles of several invariantly conserved amino acid residues [for example, see Louie and Brayer (1989), Hickey et al. (1991), Komar-Panicucci et al. (1992), and Berghuis et al. (1994a,b)]. While cytochrome *c* provides an appropriate paradigm for the examination of questions of structure−function and structure−stability relationships, these questions are obviously also of broader interest [for example, see Wells (1990), Mildvan et al. (1992), and Matthews (1993)].

Much of the work directed at cytochrome *c* involves gaining a quantitative understanding of the factors governing the maintenance of the heme reduction potential. The reduction potentials of eukaryotic cytochromes *c* are remarkably similar (270 ± 20 mV), presumably as a functional requirement for electron transfer both to and from their mitochondrial redox partners. The conserved residues Arg38, Asn52, and Phe82 have been extensively studied to determine both their individual (Cutler et al., 1989; Rafferty et al., 1990) and combined (Komar-Panicucci et al., 1992) contributions to the reduction potential of cytochrome *c*. Figure 1 illustrates the spatial placement of these residues within the structure of yeast iso-1 cytochrome *c* and shows that each is distally located (>9 Å) from the others. Arginine 38 is a partially buried residue involved in a hydrogen-bonding network with propionate A of the heme group and two conserved internal water molecules (Louie & Brayer, 1990). Substitution by an alanine both removes a positively charged side chain and creates an access point to bulk solvent, resulting in a significant decrease in the midpoint reduction potential of this protein (Cutler et al., 1989). Asparagine 52 is a completely internal residue which is part of a hydrogen-bonding network involving the conserved internal water molecule Wat166, which appears to be an important component in the structural transition between oxidation states in cytochrome *c* (Berghuis & Brayer, 1992). Mutation of this residue to an isoleucine dramatically increases thermodynamic stability (Das et al., 1989; Hickey et al., 1991) and acts to decrease the observed reduction

[†] These studies were supported by grants from the Medical Research Council of Canada (to G.D.B.), the National Institutes of Health (to G.M.), and the National Science Foundation (to F.S. and G.M.). T.P.L. is the recipient of a Studentship from the MRC of Canada.

[‡] Atomic coordinates for the structures discussed herein have been deposited with the Protein Data Bank as entries 1CIE (N52I/F82S), 1CIF (R38A/F82S), 1CIG (R38A/N52I), and 1CIH (R38A/N52I/F82S).

* Author to whom correspondence should be addressed.

[§] University of British Columbia.

[||] Department of Chemistry, University of Rochester.

[⊥] Departments of Biochemistry and Biophysics, University of Rochester.

[⊗] Abstract published in *Advance ACS Abstracts,* March 1, 1995.

0006-2960/95/0434-5259$09.00/0 

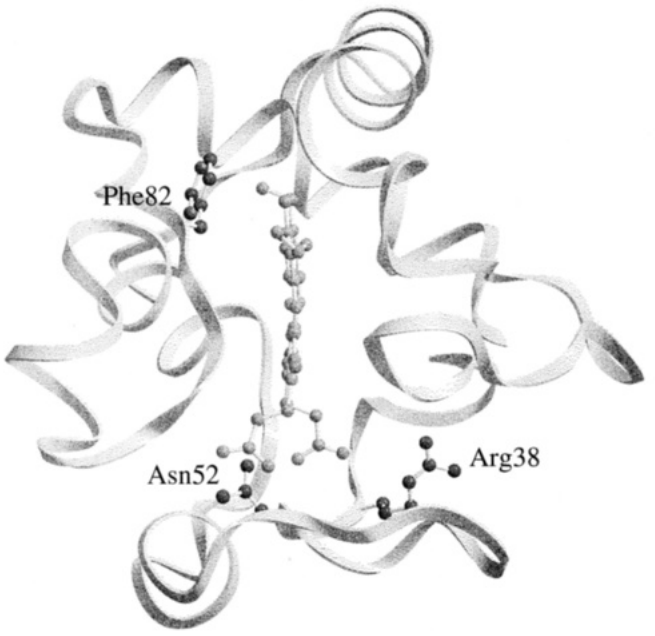


FIGURE 1: Ribbon representation of the polypeptide chain backbone of wild-type yeast iso-1 cytochrome *c* showing the relative positions of the three mutation sites at Arg38, Asn52, and Phe82. A ball-and-stick representation is used to show the heme group (light shading) and the side chains of Arg38, Asn52, and Phe82 (dark shading).

potential (Guillemette et al., 1994). The major structural alteration in the N52I mutant protein is the exclusion of Wat166 and an adjustment of internal hydrogen bonding (Berghuis et al., 1994a). Phenylalanine 82 is a residue with one edge of its planar side chain exposed on the surface of cytochrome *c* and the other buried in the hydrophobic heme pocket. This residue is critical to the maintenance of the heme pocket and the exclusion of solvent from access to the central heme group. Replacement of Phe82 by a serine has a dramatic effect on both the electrochemical properties (Rafferty et al., 1990) and the structure (Louie et al., 1988b) of yeast iso-1 cytochrome *c*.

The goal of the current studies is to gain further insight into the roles of Arg38, Asn52, and Phe82 and determine whether synergistic effects on structure, with subsequent modification of reduction potentials, are observed in cytochrome *c* when more than one of these residues is mutated at a time. In this way, questions pertaining to overlapping roles of these highly conserved residues can be addressed. For this purpose, mutant proteins containing all possible combinations of the three mutations R38A, N52I, and F82S have been examined at high resolution using X-ray diffraction methods and the cumulative effects of these distal mutations on the structure of cytochrome *c* have been studied. The further availability of the structures of the three single mutant proteins (Louie et al., 1988b; Berghuis et al., 1994a; H. Tong, personal communication) provides a standard against which our structural analyses can be compared.

## EXPERIMENTAL PROCEDURES

Mutants of yeast iso-1 cytochrome *c* with combinations of the R38A, N52I, and F82S substitutions were constructed, expressed, and purified as previously described (Komar-Panicucci et al., 1992). All mutant cytochromes *c* were produced with the naturally occurring cysteine at position 102 replaced by alanine in order to prevent the formation of covalent homodimers.

Table 1: Data Collection Parameters

| | iso-1 cytochrome *c* mutant | | | |
|---|---|---|---|---|
| parameter | R38A/ N52I | R38A/ F82S | N52I/ F82S | R38A/ N52I/R82S |
| space group | $P4_32_12_1$ | $P4_32_12$ | $P4_32_12$ | $P4_32_12$ |
| cell dimensions (Å) | | | | |
| $a = b$ | 36.42 | 36.75 | 36.10 | 36.48 |
| $c$ | 137.03 | 137.39 | 137.47 | 137.28 |
| resolution (Å) | 1.8 | 1.8 | 1.6 | 1.8 |
| frames collected | 45 | 39 | 78 | 130 |
| reflns measured | 19 351 | 22 149 | 40 973 | 71 744 |
| unique reflns | 6667 | 7030 | 9777 | 8999 |
| merging *R*-factor[a] | 0.067 | 0.091 | 0.056 | 0.064 |

[a] Merging *R*-factor = $\dfrac{\sum_{hkl}\sum_{i=0}^{n}|I_{i_{hkl}} - \bar{I}_{hkl}|}{\sum_{hkl}\sum_{i=0}^{n} I_{i_{hkl}}}$

Crystals of each reduced yeast iso-1 cytochrome *c* mutant protein were grown from a solution of 88% ammonium sulfate and 70 mM sodium dithionite buffered at pH 6.5 by 0.1 M sodium phosphate. These conditions are similar to those used to grow diffraction quality crystals of the wild-type protein (Sherwood & Brayer, 1985; Louie et al., 1988a). The hanging drop vapor diffusion method was employed with seeding from either micro- or macrocrystals (Leung et al., 1989). Mutant protein crystals are of the space group $P4_32_12$ with unit cell dimensions as indicated in Table 1 and are isomorphous with crystals of wild-type yeast iso-1 cytochrome *c*.

For each of the four mutant cytochromes *c*, X-ray diffraction data were collected on a Rigaku R-AXIS II imaging plate area detector from a single crystal. The incident radiation was provided by an RU-300 rotating-anode generator operating at 90−100 mA and 50−60 kV. For each frame, each crystal was oscillated through a $\phi$ angle of 1.0° and exposed to the X-ray beam for 20−30 min. X-ray intensity data were processed to structure factors (summarized in Table 1) using the R-AXIS II data processing software (Higashi, 1990; Sato et al., 1992). The R38A/F82S and N52I/F82S crystals diffracted only weakly beyond 1.9- and 1.8-Å resolution, respectively, so diffraction intensities exceeding these limits were not used in subsequent data processing and refinement. Each mutant protein data set was put on an absolute scale using the Wilson (1942) plot method.

The restrained parameter least-squares approach (Hendrickson, 1985) was employed for the refinement of each cytochrome *c* mutant structure. Starting models for structural refinement were based on the high-resolution structure of wild-type iso-1 cytochrome *c* (Louie & Brayer, 1990). All mutated residues were initially modeled as alanines. The side chains of these residues were fitted into $F_o - F_c$ and $2F_o - F_c$ difference electron density maps early in refinement. Mutation of Arg38 to alanine was confirmed by the lack of electron density at the original side-chain position. Mutation of Asn52 to isoleucine was clearly evident in those proteins with this replacement and was accompanied by the concomitant elimination of the internal water molecule, Wat166. In those mutant proteins where Phe82 was replaced by serine, electron density maps clearly showed the position of the serine hydroxyl group in addition to the position of a newly bound water molecule. Also included in the starting

Table 2: Refinement Parameters

| parameter | iso-1 cytochrome *c* mutant R38A/N52I | R38A/F82S | N52I/F82S | R38A/N52I/F82S |
|---|---|---|---|---|
| resolution range (Å) | 6.0−1.8 | 6.0−1.9 | 6.0−1.8 | 6.0−1.8 |
| data cutoff | $3\sigma(F)$ | $2\sigma(F)$ | $3\sigma(F)$ | $3\sigma(F)$ |
| no. of reflns used | 6309 | 6018 | 7706 | 8587 |
| no. of protein atoms | 886 | 881 | 887 | 881 |
| no. of solvent atoms | 75 | 80 | 70 | 73 |
| av thermal factors (Å$^2$) | | | | |
| protein atoms | 22.5 | 21.0 | 21.2 | 23.8 |
| solvent atoms | 34.4 | 29.0 | 34.5 | 36.7 |
| *R*-factor[a] | 0.189 | 0.198 | 0.197 | 0.199 |

[a] $R\text{-factor} = \sum|F_o - F_c|/\sum|F_o|$.

Table 3: Stereochemical Parameters for Refined Mutant Protein Structures

| stereochemical parameter | rms deviation from ideal values R38A/N52I | R38A/F82S | N52I/F82S | R38A/N52I/F82S | restraint weight |
|---|---|---|---|---|---|
| distances (Å) | | | | | |
| bond (1−2) | 0.019 | 0.019 | 0.019 | 0.019 | 0.020 |
| angle (1−3) | 0.039 | 0.039 | 0.038 | 0.039 | 0.030 |
| planar (1−4) | 0.050 | 0.046 | 0.047 | 0.049 | 0.045 |
| planes (Å) | 0.014 | 0.014 | 0.014 | 0.014 | 0.018 |
| chiral volumes (Å$^3$) | 0.141 | 0.148 | 0.133 | 0.156 | 0.120 |
| nonbonded contacts (Å)[a] | | | | | |
| single torsion | 0.211 | 0.211 | 0.218 | 0.211 | 0.250 |
| multiple torsion | 0.198 | 0.194 | 0.186 | 0.193 | 0.250 |
| possible hydrogen bonds | 0.201 | 0.227 | 0.207 | 0.183 | 0.250 |
| torsion angles (deg) | | | | | |
| planar (0° or 180°) | 2.3 | 2.2 | 2.2 | 2.5 | 2.5 |
| staggered (±60°, 180°) | 22.0 | 21.9 | 21.1 | 18.5 | 20.0 |
| orthonormal (±90°) | 20.8 | 20.6 | 21.3 | 25.0 | 15.0 |

[a] The rms deviations from ideality for this class of restraint incorporate a reduction of 0.2 Å from the radius of each atom involved in a contact.

models were all water molecules from the wild-type structure having isotropic thermal factors below 50 Å$^2$, with the exception of those in the vicinity of residues 38, 52, and 82. All water molecules were refined as fully occupied neutral oxygen atoms. Also included in refinement was a sulfate anion bound to the amino-terminal end of the N-terminal helix of cytochrome *c*.

Omit, $F_o - F_c$, and $2F_o - F_c$ difference electron density maps covering the entire course of the polypeptide chain were examined periodically during the course of least-squares refinement. These resulted in a number of manual corrections of surface side-chain positions, as well as the identification of additional water molecules and the deletion of a number of weakly resolved water molecules. Water molecules considered for inclusion into the model were found by the use of an iterative procedure involving alternating rounds of peak searching and reciprocal space refinements (Tong et al., 1994). Final refinement parameters for all four mutant protein structures are tabulated in Table 2. The final stereochemistry of these structures is summarized in Table 3.

Atomic coordinate errors for each of the four mutant protein structures have been estimated using two methods. Inspection of a Luzzati (1952) plot (Figure 2) provides estimates of rms coordinate errors ranging from 0.18 Å for the R38A/N52I structure to 0.22 Å for the R38A/F82S structure. The N52I/F82S and R38A/N52I/F82S structures both have rms coordinate errors of 0.20 Å by this method.

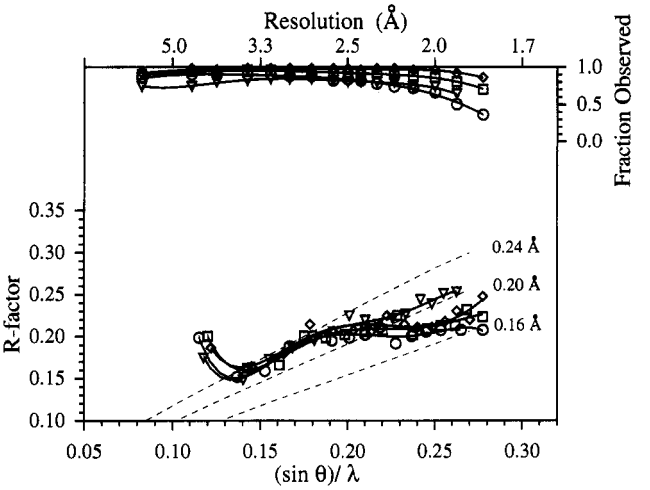


FIGURE 2: Plot of crystallographic *R*-factor as a function of resolution at the end of refinement for the R38A/N52I (○), R38A/F82S (▽), N52I/F82S (□), and R38A/N52I/F82S (◇) mutant yeast iso-1 cytochromes *c*. The theoretical dependence of the *R*-factor on resolution assuming various levels of rms error in the atomic positions of the models (Luzzati, 1952) is shown as broken lines. The fraction of theoretical data used in structural refinement is plotted at the top using the axis at the top right.

Table 4: Overall Average Positional Deviations (Å) between Mutant and Wild-Type Yeast Iso-1 Cytochromes *c*

| atom groups | iso-1 cytochrome *c* mutant R38A/N52I | R38A/F82S | N52I/F82S | R38A/N52I/F82S |
|---|---|---|---|---|
| all common protein atoms | 0.27 | 0.26 | 0.32 | 0.30 |
| all main-chain atoms | 0.19 | 0.17 | 0.22 | 0.19 |
| all common side-chain atoms | 0.38 | 0.36 | 0.44 | 0.42 |
| all heme atoms | 0.17 | 0.19 | 0.22 | 0.21 |

Overall atomic coordinate errors can also be estimated by evaluating individual atomic errors (Cruickshank, 1949, 1954). Based on this method, the estimated overall rms coordinate errors are 0.13 Å for the R38A/N52I structure, 0.14 Å for the R38A/F82S structure, and 0.12 Å for the N52I/F82S and R38A/N52I/F82S structures.

## RESULTS

*Structural Comparison of Mutant and Wild-Type Cytochromes c.* The overall fold of the polypeptide chain in all four proteins with mutations at distal sites is very similar to that observed for wild-type yeast iso-1 cytochrome *c* (Table 4). The distribution of average positional deviations over the course of the polypeptide chain is shown for each of these mutant cytochromes *c* in Figure 3. Larger variations in the positions of the N-terminal residues Thr(−5) through Phe(−3) arise as a consequence of thermal disorder in this region of the protein (Louie & Brayer, 1990) rather than as a consequence of the introduced mutations. In addition, the hydrophilic side chains of Lys(−2), Lys4, Glu21, Glu44, Lys54, Lys55, Asn63, Glu66, Lys86, Lys87, Lys89, and Lys100 are all on the surface of the protein and are projected out into the surrounding solvent medium. As such, these side chains are substantially disordered and display large positional deviations between the various structures studied. Three hydrophobic residues on the protein surface also undergo apparent positional shifts, but these changes arise from either the presence of multiple residue conformations (Leu9), the high mobility of the local polypeptide backbone

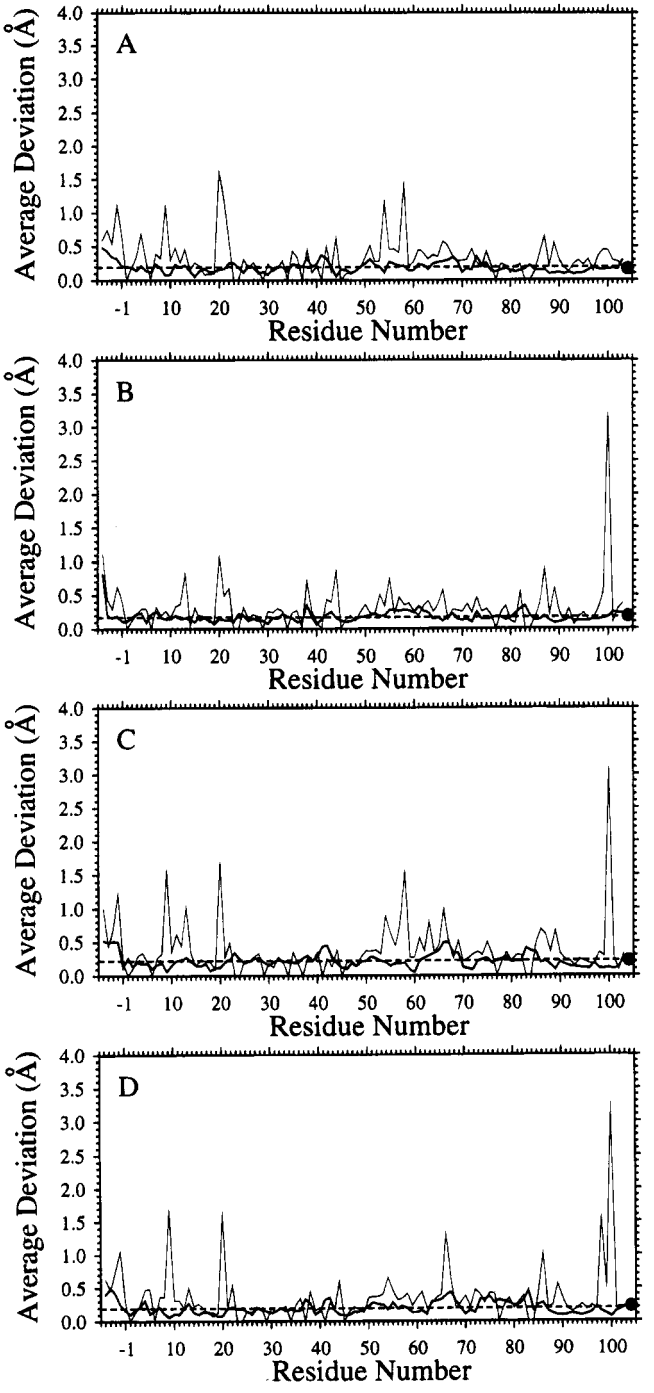


FIGURE 3: Plots of average positional deviations from wild-type iso-1 cytochrome *c* along the course of the polypeptide chain for the (A) R38A/N52I, (B) R38A/F82S, (C) N52I/F82S, and (D) R38A/N52I/F82S mutant proteins. Thick lines indicate average deviations of main-chain atoms, while thin lines indicate average deviations of the equivalent side-chain atoms. In each diagram, the filled circle at residue position 104 represents the average positional deviation of the heme group and the horizontal dashed line represents the average positional deviation for all main-chain atoms (Table 4).

(Val57), or a combination of these factors (Leu58). These three residues display similar characteristics in wild-type yeast iso-1 cytochrome *c* (Louie & Brayer, 1990).

Examination of the heme geometry of the mutant proteins (Table 5) reveals that all four proteins are comparable to the wild-type protein in this regard. Of note is the shorter than expected ligand distance between the NE2 atom of His18 and the heme iron atom in the N52I/F82S protein.

Table 5: Heme Geometry of Mutant and Wild-Type Yeast Iso-1 Cytochromes *c*[a]

| | wild type | R38A/ N52I | R38A/ F82S | N52I/ F82S | R38A/ N52I/F82S |
|---|---|---|---|---|---|
| (1) Angular Deviations (deg) between the Pyrrole Nitrogen Plane Normal and the Four Individual Pyrrole Ring Plane Normals and the Heme Coordinate Bonds | | | | | |
| A | 9.4 | 12.7 | 16.0 | 11.4 | 9.4 |
| B | 11.1 | 10.5 | 11.4 | 9.0 | 8.3 |
| C | 8.8 | 10.6 | 12.3 | 10.9 | 8.2 |
| D | 8.1 | 10.9 | 13.2 | 9.1 | 10.1 |
| Fe−His18 NE2 | 2.2 | 2.3 | 4.2 | 7.2 | 1.5 |
| Fe−Met80 SD | 4.9 | 4.2 | 1.4 | 3.4 | 3.4 |
| (2) Angular Deviations (deg) between the Porphyrin Ring Plane Normal and the Four Pyrrole Ring Plane Normals, the Pyrrole Nitrogen Plane Normal, and the Heme Coordinate Bonds | | | | | |
| A | 6.7 | 9.1 | 11.9 | 6.7 | 5.3 |
| B | 11.9 | 12.4 | 14.8 | 10.7 | 9.1 |
| C | 9.8 | 11.0 | 11.4 | 10.4 | 9.3 |
| D | 6.0 | 7.6 | 9.1 | 4.4 | 6.0 |
| NNNN | 2.6 | 4.0 | 4.8 | 4.7 | 4.1 |
| Fe−His18 NE2 | 3.2 | 3.3 | 4.5 | 2.8 | 2.7 |
| Fe−Met80 SD | 7.5 | 7.3 | 5.6 | 7.2 | 7.5 |
| (3) Bond Distances (Å) between the Heme Iron Atom and Its Six Ligands | | | | | |
| His18 NE2 | 1.98 | 1.91 | 1.96 | 1.80 | 1.94 |
| Met80 SD | 2.36 | 2.33 | 2.39 | 2.33 | 2.38 |
| heme NA | 1.97 | 1.99 | 1.97 | 2.00 | 1.99 |
| heme NB | 2.00 | 2.01 | 2.01 | 2.00 | 2.04 |
| heme NC | 1.99 | 2.01 | 2.03 | 1.98 | 2.03 |
| heme ND | 2.01 | 2.05 | 2.02 | 2.08 | 2.04 |

[a] The pyrrole nitrogen plane is defined by the four pyrrole nitrogens of the heme group. The four pyrrole ring planes are each defined by the five atoms of the ring and the first carbon atom attached to each of the four carbons of the ring. The porphyrin ring is defined by the five atoms in each of the four pyrrole rings, the four bridging methine carbon atoms, the first carbon atom of each of the eight side chains of the heme, and the central iron atom of the heme. The heme atom nomenclature used in this table follows the conventions of the Protein Data Bank [see Figure 3 of Berghuis and Brayer (1992)].

This apparently arises from movement of the side chain of His18 toward the heme group ($\Delta d$ = 0.2 Å) and leads to a perturbation of the angle between this bond and the pyrrole nitrogen plane (the angle becomes ~7.2° instead of the average of ~2.6°; Table 5).

In order to avoid homodimer formation, all four mutant proteins had the additional substitution of Cys102 by alanine. The site of this mutation is distant from those of the others and has previously been shown to have no functional implications (Hickey et al., 1991). In the present structural studies, this mutation has no effect on the course of the polypeptide chain (Figure 3). In the local vicinity, the only conformational change observed is in the side chain of Val20, which shifts toward the newly available space near Ala102 ($\Delta d$ = 1.1−1.7 Å). Except for a complementary movement of the Leu98 side chain ($\Delta d$ = 1.6 Å) in the R38A/N52I/F82S mutant, no other structural effects are seen in this region of the protein. A further comparison of these four multiple-mutant proteins with the structures of their single-site-mutant counterparts which have either a cysteine, threonine, or alanine residue at position 102 also indicates that there are negligible effects on the local structure of the protein.

*R38A Mutation Site.* The replacement of Arg38 by an alanine represents a substantial decrease in side-chain size as well as the elimination of a positive charge located partially in the interior of the protein in close proximity to

Table 6: Heme Propionate Hydrogen Bond Interactions in Mutant and Wild-Type Yeast Iso-1 Cytochromes *c*[a]

| | distances (Å) | | | | | | | |
|---|---|---|---|---|---|---|---|---|
| interaction | wild-type | R38A[b] | N52I[c] | F82S[d] | R38A/N52I | R38A/F82S | N52I/F82S | R38A/N52I/F82S |
| Heme O1A−Tyr48 OH | 2.81 | 2.89 | 2.63 | 2.92 | 2.85 | 3.10 | 2.74 | 2.57 |
| −Wat121 | 2.81 | 2.58 | 3.48 | 2.88 | 2.86 | 3.47 | 2.70 | 2.72 |
| −Wat168 | 2.84 | 3.18 | 3.50 | 3.10 | 3.34 | 3.42 | 3.16 | 3.18 |
| Heme O2A−Gly41 N | 3.21 | 3.02 | 3.07 | 2.90 | 3.26 | 3.06 | 3.01 | 3.07 |
| −Asn52 ND2 | 3.33 | 3.30 | | 2.70 | | 3.37 | | |
| −Trp59 NE1 | 3.10 | 2.88 | 2.84 | (3.71) | 2.90 | 3.08 | 2.94 | 3.11 |
| −Wat121 | (4.01) | (3.50) | (3.91) | (3.70) | (3.91) | (4.22) | (3.75) | (3.57) |
| Heme O1D−Thr49 N | 2.94 | 2.72 | 2.79 | 3.07 | 2.92 | 2.72 | 2.81 | 2.90 |
| Heme O2D−Thr49 OG1 | 2.64 | 2.56 | 2.49 | 3.16 | 2.72 | 2.76 | 2.53 | 2.61 |
| −Thr78 OG1 | 2.90 | 3.11 | 2.76 | (3.67) | 2.86 | 3.01 | 2.74 | 2.81 |
| −Lys79 N | 3.18 | 2.95 | 3.03 | 3.01 | 3.09 | 3.13 | 3.02 | 3.10 |
| Wat121−Arg38 NE | 2.81 | | 2.97 | (3.72) | | | 3.11 | |
| −Wat168 | (3.55) | (4.31) | (4.17) | (4.67) | (4.23) | (4.92) | (3.77) | (4.10) |
| −WatA[e] | | (3.92) | | | 2.55 | 2.47 | | 3.24 |
| Wat168−Arg38 NH1 | 2.56 | | 2.93 | 3.33 | | | 2.65 | |
| −WatB[e] | | 3.22 | | | 2.90 | 2.74 | | |
| WatA[e]−WatB[e] | | 2.91 | | | 2.64 | 2.79 | | |

[a] Values listed are the distances between hydrogen donor and acceptor atoms. Values given in parentheses are not considered to be hydrogen bonds but are listed for comparison. [b] From H. Tong, unpublished results. [c] From Berghuis et al. (1994a). [d] From Louie et al. (1988b). [e] WatA and WatB are the water molecules which replace the Arg38 side chain and are closest to Wat121 and Wat168, respectively.

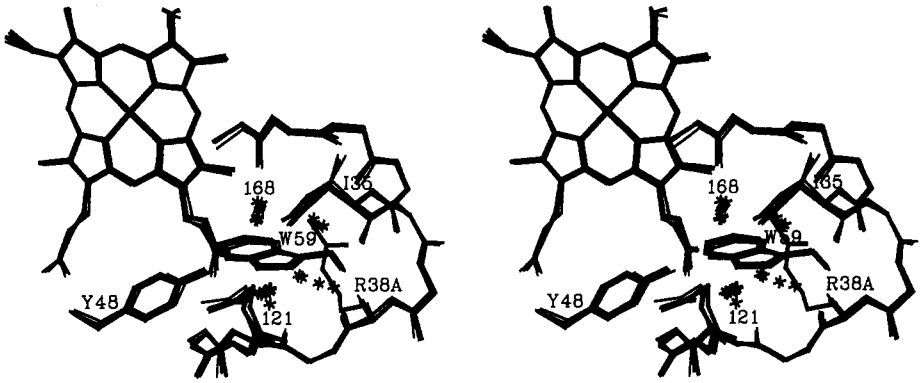


FIGURE 4: Stereodiagram of the region around the R38A mutation site in iso-1 cytochrome *c*. The structures of the R38A, R38A/N52I, R38A/F82S, and R38A/N52I/F82S mutant proteins are all drawn with thin lines and superimposed on the structure of the wild-type protein (thick lines). Water molecules are shown as asterisks, with the two conserved water molecules, Wat121 and Wat168, labeled.

the heme propionate A group. The space vacated by the Arg38 side chain is filled by two water molecules (Wat A and B) which serve to maintain the structure of the hydrogen-bonding network centered around heme propionate A (Table 6; Figure 4). In the R38A/N52I/F82S mutant protein only Wat A is present. These water molecules form a solvent channel into the interior of the protein, thereby directly exposing the O1A atom of heme propionate A to the external solvent medium. Spatially, these new water molecules are located at positions comparable to the NE and NH1 atoms of Arg38 and participate in similar hydrogen-bonding interactions with two conserved water molecules, Wat121 and Wat168 (Table 6). In turn, the conserved Wat121 and Wat168 retain positions comparable to those found in the wild-type protein and form hydrogen bonds to the O1A atom of heme propionate A.

*N52I Mutation Site.* Substitution of Asn52 by isoleucine involves the exchange of a polar side chain for a nonpolar side chain of approximately equivalent size but of different shape. In the N52I single site mutant protein, the highly conserved internal water molecule, Wat166, is excluded from the protein. In addition, the side chain of Tyr67 moves away from the side chain of Met80 ($\Delta d = 0.6$ Å) and toward that of Thr78, forming a new hydrogen bond interaction (Table 7; Figure 5; Berghuis et al., 1994a). These changes are observed in all of the combinatorial mutant proteins having the N52I mutation (Table 7; Figure 5), with the Tyr67 side chain undergoing a positional shift of 0.5−0.6 Å.

*F82S Mutation Site.* The mutation of Phe82 to serine brings about the creation of a solvent channel directly into the heme pocket, thereby disrupting the nonpolar environment of the heme and leading to a significant drop in the reduction potential of cytochrome *c* (Louie et al., 1988b). In the combination mutants containing the F82S mutation, a comparable phenomenon is observed, with a single water molecule being observed in the newly created solvent channel (Figure 6) and a significant increase in the solvent exposure of the heme porphyrin ring (Table 8; Louie et al., 1988b). As is apparent from Table 8, increased heme solvent exposure is caused solely by the F82S mutation and is not affected by either the R38A or the N52I mutation.

The side chain of Arg13 is in the vicinity of the F82S mutation site and shows considerable variability in the conformations adopted in the different combinatorial mutants (Figure 6). Nonetheless, the Arg13 side chain occupies the same general surface region in each case, and the variability observed for this residue likely arises from the high thermal factors observed for this side chain (32.4 Å$^2$ in the wild-

Table 7: Wat166 Hydrogen Bond Interactions in Mutant and Wild-Type Yeast Iso-1 Cytochromes *c*[a]

| | distances (Å) | | | | | | | |
|---|---|---|---|---|---|---|---|---|
| interaction | wild-type | R38A[b] | N52I[c] | F82S[d] | R38A/N52I | R38A/F82S | N52I/F82S | R38A/N52I/F82S |
| Wat166−Asn52 ND2 | 3.14 | (3.72) | | (4.13) | | 3.21 | | |
| −Tyr67 OH | 2.62 | 2.60 | | 2.36 | | 2.46 | | |
| −Thr78 OG1 | 2.72 | 2.53 | | 2.89 | | 2.90 | | |
| Tyr67 OH−Thr78 OG1 | (4.18) | (4.21) | 3.41 | (3.73) | 3.45 | (4.10) | 3.42 | 3.31 |
| −Met80 SD | 3.25 | 3.19 | (3.63) | 3.02 | (3.61) | 3.26 | (3.40) | (3.60) |

[a] Values listed are the distances between hydrogen donor and acceptor atoms. Values given in parentheses are not considered to be hydrogen bonds but are listed for comparison. [b] From H. Tong, unpublished results. [c] From Berghuis et al. (1994a). [d] From Louie et al. (1988b).

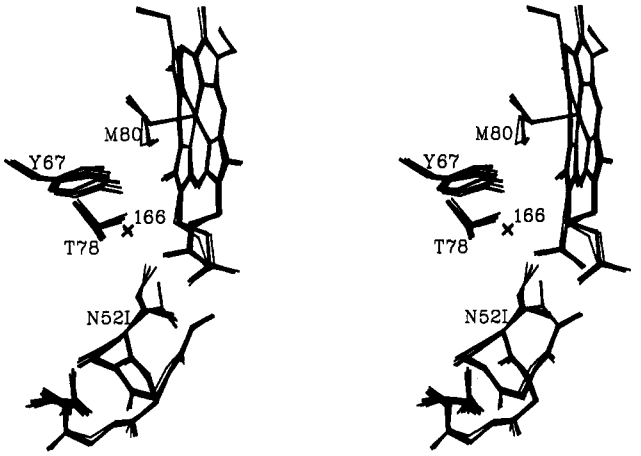


FIGURE 5: Stereodiagram of the region around the N52I mutation site in iso-1 cytochrome *c*. The structures of the N52I, R38A/N52I, N52I/F82S, and R38A/N52I/F82S mutant proteins are all drawn with thin lines and superimposed on the structure of the wild-type protein (thick lines). An internally bound water molecule found only in the wild-type protein and located adjacent to Asn52, Tyr67, and Thr78 is represented by an asterisk.

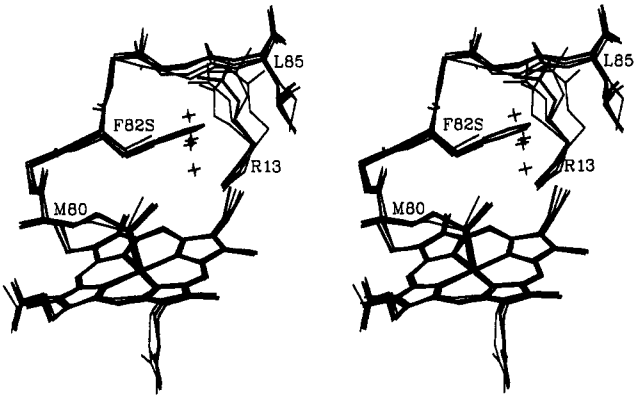


FIGURE 6: Stereodiagram of the region around the F82S mutation site in iso-1 cytochrome *c*. The structures of the F82S, R38A/F82S, N52I/F82S, and R38A/N52I/F82S mutants are all drawn with thin lines and superimposed on the structure of the wild-type protein (thick lines). Water molecules bound in the solvent channel formed by the replacement of phenylalanine by serine at position 82 are shown as asterisks.

type protein; Louie & Brayer, 1990; average $B$ is 38.4 Å$^2$ in F82S mutants).

A further structural change is an increase in thermal parameters for residue 82 and the two glycines at positions 83 and 84 (Figure 7; average $B$ of these three residues is 17.1 Å$^2$ in wild-type and 32.2 Å$^2$ averaged over F82S mutants). This increase in thermal parameters is particularly marked for the N52I/F82S ($\Delta B$ = +14.8 Å$^2$) and R38A/N52I/F82S ($\Delta B$ = +18.1 Å$^2$) mutants (Figure 7). Increased mobility likely arises from the loss of the tight packing interactions formed by the aromatic ring of Phe82, which is sandwiched between this segment of polypeptide chain and the heme group. Another factor is that the water molecule introduced into the newly formed solvent channel at residue 82 can form a hydrogen bond to the carbonyl oxygen of Leu68 ($d$ = 3.2 Å) and thereby interfere with the hydrogen bond normally found between this latter group and the main-chain nitrogen atom of Leu85. This would allow more freedom of motion for the flexible Gly83−Gly84 segment of the polypeptide chain. Comparison of the thermal parameters for the F82S single mutant and the wild-type protein is not conclusive, probably due to the relatively low resolution (2.8 Å) of the structural determination for this mutant protein (Louie et al., 1988b).

*The Conserved Internal Water, Wat166.* In all eukaryotic cytochromes *c* examined thus far, a conserved water molecule is centrally located and hydrogen bonded to Asn52, Tyr67, and Thr78 (Bushnell et al., 1990). A shift in the position of Wat166 toward the heme iron atom is observed in the structure of the oxidized form of yeast iso-1 ($\Delta d$ = 1.7 Å) and other cytochromes *c* (Berghuis & Brayer, 1992). This oxidation state dependent shift results in the loss of the hydrogen bond between Wat166 and the side chain of Asn52. Similar structural changes are observed in both the reduced R38A (H. Tong, personal communication) and the reduced F82S mutant protein (Louie et al., 1988b), suggesting that these structures shift toward the structure of the oxidized state. In the present study, all of the protein structures determined were in the reduced state. Since the N52I mutation eliminates Wat166 from the protein interior, the only protein in the present study which retains this water molecule is the R38A/F82S double mutant. Surprisingly, Wat166 in the R38A/F82S protein does not move from the position it occupies in the reduced wild-type structure, and it retains a hydrogen bond with Asn52 (Table 7).

## DISCUSSION

The site-directed mutagenesis technique provides the opportunity to specifically make multiple site mutations within a single protein. This can be useful in determining the extent of synergistic functional and structural changes which arise from the interaction of individual mutations. In the present work, we have studied the effects of introducing mutations at three distally separated sites of yeast iso-1 cytochrome *c* involving the invariant residues Arg38, Asn52, and Phe82. At these three residues, all four possible combinatorial mutant proteins were made with the three single replacements R38A, N52I, and F82S. Our studies show that the degree of synergism between mutation sites can be quite different depending on the particular functional or structural aspect being assessed.

Table 8: Heme Solvent Accessibility in Mutant and Wild-Type Yeast Iso-1 Cytochromes *c*[a]

| | yeast iso-1 cytochrome *c* structure | | | | | | | |
|---|---|---|---|---|---|---|---|---|
| | wild-type | R38A[b] | N52I[c] | F82S[d] | R38A/N52I[b] | R38A/F82S[b] | N52I/F82S | R38A/N52I/F82S[b] |
| (1) solvent-accessible heme atoms and surface area exposed (Å$^2$) | | | | | | | | |
| CBB | 0.0 | 0.0 | 0.0 | 15.4 | 0.0 | 12.7 | 7.6 | 11.8 |
| CHD | 2.9 | 2.6 | 2.3 | 3.6 | 3.6 | 3.8 | 0.0 | 2.2 |
| CMC | 9.2 | 10.2 | 13.2 | 13.1 | 9.3 | 10.4 | 11.8 | 13.2 |
| CAC | 3.4 | 2.6 | 2.6 | 3.4 | 3.1 | 3.6 | 4.8 | 3.7 |
| CBC | 20.1 | 19.9 | 20.1 | 21.2 | 19.4 | 18.8 | 18.4 | 19.4 |
| CMD | 10.8 | 11.3 | 9.8 | 11.4 | 10.7 | 10.5 | 11.1 | 9.7 |
| (2) total heme exposure (Å$^2$) | 46.4 | 46.6 | 48.0 | 68.1 | 46.1 | 59.8 | 53.7 | 60.0 |
| (3) total heme surface (Å$^2$) | 513.1 | 516.2 | 521.2 | 511.8 | 513.0 | 512.2 | 514.6 | 510.6 |
| (4) heme surface area exposed (%) | 9.0 | 9.0 | 9.2 | 13.3 | 9.0 | 11.7 | 10.4 | 11.8 |

[a] Solvent-exposed areas were calculated by the method of Connolly (1983) with a probe sphere of 1.4-Å radius. [b] For all mutant proteins having the R38A mutation, Wat121 and Wat168 were considered an integral part of the protein structure. Results for the R38A single-mutant protein were provided by H. Tong (personal communication). [c] From Berghuis et al. (1994a). [d] From Louie et al. (1988b).

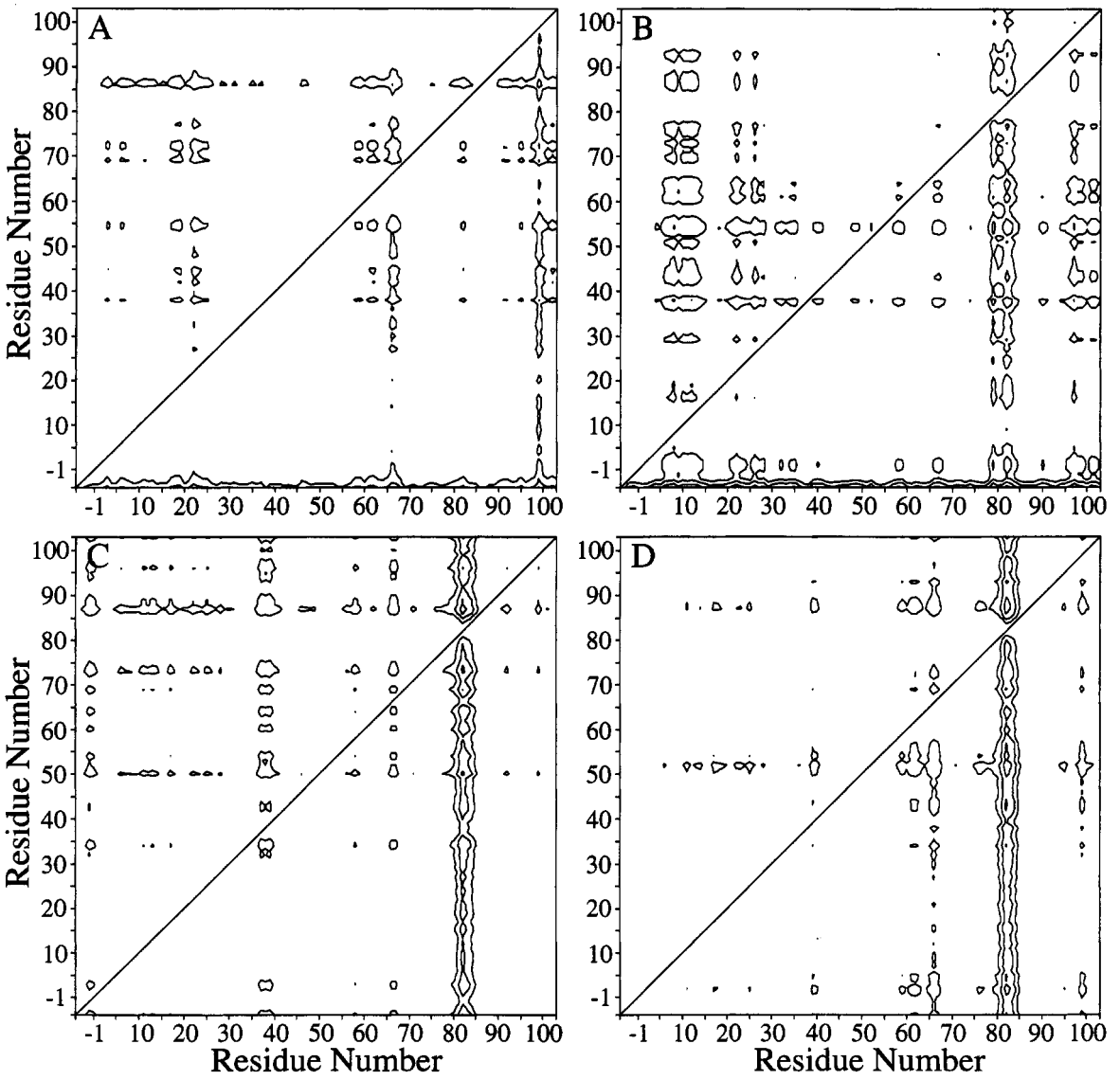


FIGURE 7: Thermal factor difference matrices from the comparison of wild-type iso-1 cytochrome *c* with the (A) R38A/N52I, (B) R38A/F82S, (C) N52I/F82S, and (D) R38A/N52I/F82S mutants. Each matrix point $P_{x,y}$ represents a pairing of amino acids $x$ and $y$. The value of the pairing is calculated from the equation $P_{x,y} = (B_x - B_y)_{\text{mutant}} - (B_x - B_y)_{\text{wild-type}}$ where $B_i$ is the average thermal factor (Å$^2$) of the main-chain atoms of a given amino acid $i$. Positive matrix values are contoured at intervals of 5 Å$^2$. Due to the inverse symmetry of the matrix across the diagonal, negative values are redundant and have been omitted. Amino acids producing vertical streaks within the matrix have significantly higher main-chain thermal factors in the mutant structure relative to the wild-type structure, while horizontal streaks indicate significantly lower main-chain thermal factors in the mutant protein.

*Structural Effects.* The replacement amino acids all represent substantial changes in side-chain character, and therefore it is not surprising that the introduction of each of these individual mutations into yeast iso-1 cytochrome *c* leads

Table 9: Unfolding of Mutant and Wild-Type Yeast Iso-1 Cytochromes *c* by Guanidine Hydrochloride

| cytochrome *c* | $C_m$ [Gdn-HCl][a] (±0.1 M) | *m* | $\Delta G°$ [b] (kcal/mol) |
|---|---|---|---|
| wild-type | 1.3 | 3.8 | 4.9 |
| R38A | 1.4 | 3.4 | 4.8 |
| N52I | 2.1 | 4.2 | 9.0 |
| F82S | 0.9 | 3.8 | 3.4 |
| R38A/N52I | 2.1 | 3.8 | 8.2 |
| R38A/F82S | 0.8 | 3.4 | 2.7 |
| N52I/F82S | 1.7 | 3.4 | 5.6 |
| R38A/N52I/F82S | 1.7 | 3.6 | 6.2 |

[a] Midpoints of unfolding by guanidine hydrochloride were taken from Komar-Panicucci et al. (1992). [b] $\Delta G°$ ≡ free energy extrapolated to 0 M [Gdn-HCl]; $\Delta G° = mC_m$.

Table 10: Reduction Potentials for Mutant and Wild-Type Yeast Iso-1 Cytochromes *c*[a]

| cytochrome *c* | $E_m$ (mV)[b] | $\Delta E_m$ (mV) | expected $\Delta E_m$ (mV)[c] |
|---|---|---|---|
| wild type | 285 ± 2 | | |
| R38A | 239 ± 2 | −46 | |
| N52I | 231 ± 2 | −54 | |
| F82S | 247 ± 2 | −38 | |
| R38A/N52I | 212 ± 2 | −73 | −100 |
| R38A/F82S | 203 ± 2 | −82 | −84 |
| N52I/F82S | 189 ± 2 | −96 | −92 |
| R38A/N52I/F82S | 162 ± 2 | −123 | −111 to −142[d] |

[a] Experimental conditions were 25 °C, pH 7.0, and $\mu$ = 0.1 M. Values are listed relative to a standard hydrogen electrode reference. [b] From Komar-Panicucci et al. (1992). [c] Based on a simple numerical addition of the effects of individual mutations. [d] Range of values obtained by combining the various midpoint potentials observed for single- and double-site mutant proteins.

to significant structural and functional changes (Louie et al., 1988b; Hickey et al., 1991; Berghuis et al., 1994a). The structural consequences of each mutation in the combinatorial mutant proteins are similar to those previously observed in the single-mutant proteins (Louie et al., 1988b; Berghuis et al., 1994a). In general, the structural effects of each mutation are independent of the effects arising from mutations made at the other two sites. Thus for this set of mutant proteins with multiple distal substitutions, the structural effects observed do not have a synergistic component.

*Protein Stability.* In terms of stability to guanidine hydrochloride denaturation (Komar-Panicucci et al., 1992), the effect of individual mutation sites can be understood from the structural changes observed for each. For example, one structural role of the Arg38 side chain is to provide two hydrogen-bonding groups to interact with two conserved water molecules, Wat121 and Wat168 (Table 6). These hydrogen bonds are replaced in the R38A mutant protein by the substitution of water molecules (Wat A and B) in place of the side chain of Arg38 (Table 6; Figure 4). Apparently, the maintenance of these hydrogen-bonding interactions is sufficient to preserve the structural integrity of cytochrome *c*, thereby accounting for the negligible change in protein stability observed upon the introduction of this mutation (Table 9; Komar-Panicucci et al., 1992).

The N52I mutant protein is significantly more stable than wild-type yeast iso-1 cytochrome *c* (Table 9; Komar-Panicucci et al., 1992). This effect appears to be due to several factors, including replacement of a polar side chain by one of a hydrophobic nature within the hydrophobic core of the protein (Hickey et al., 1991); displacement of an internal water molecule, Wat166 (Berghuis et al., 1994a); and realignment of the hydrogen-bonding network in this region (Table 7; Figure 5). Finally, the N52I mutation abolishes the structural transition between the reduced and oxidized states of the protein (Berghuis et al., 1994a), and this is likely an important feature in maintaining the overall stability of the protein, especially in the oxidized state (Berghuis & Brayer, 1992).

The F82S replacement destabilizes yeast iso-1 cytochrome *c* (Table 9; Komar-Panicucci et al., 1992) by the introduction of a solvent channel and a bound water molecule into the hydrophobic core of the protein (Figure 6; Louie et al., 1988b). This is evident in the increased thermal parameters in the immediate vicinity of the mutation site (Figure 7). Such changes can also account for the lowering of the thermal stability of the heme pocket in the F82S protein relative to the wild-type protein (Hildebrandt et al., 1991).

An analysis of the stability data for the four multiple-mutant proteins for which structures were determined reveals the extent to which the R38A, N52I, and F82S mutations interact in this regard (Table 9; Komar-Panicucci et al., 1992). The combination of the N52I and F82S mutations results in a net stabilization of cytochrome *c* due to the larger stabilizing contribution of the N52I replacement. This is not as large as in the N52I single-mutant protein due to the destabilizing influence of the F82S mutation. Since the R38A mutation has a neutral effect on stability, the R38A/N52I double-mutant protein has a stability similar to that of the N52I single mutant, whereas the R38A/F82S mutant protein is destabilized to the same extent as the F82S single mutant. Consistent with the stability of these double-mutant proteins, the R38A/N52I/F82S triple mutant has a stability which is essentially the same as that of the N52I/F82S double-mutant protein. Thus with respect to stability, the effects of each of the three mutations are independent and cumulative in the multiple-mutant proteins. This is a reflection of the independent nature of the structural changes induced at each individual mutation site, which are distally located.

*Reduction Potential Effects.* Each of the mutant cytochromes *c* containing multiple substitution sites has a midpoint reduction potential significantly lower than that of either the wild-type protein or the related proteins with single site substitutions (Table 10; Komar-Panicucci et al., 1992). For the R38A/F82S and N52I/F82S mutant proteins, the observed reduction potentials are similar to what would be expected if the effect of each of the single mutations were independent and additive. In contrast, the R38A/N52I mutant has a reduction potential which is significantly higher than the expected value (Table 10). The triple-mutant R38A/N52I/F82S protein has the lowest reduction potential observed, with a measured value which falls approximately midway within the range of values expected by combining the various reduction potentials observed for single- and double-site mutant proteins.

The higher than expected reduction potential observed for the R38A/N52I double-mutant cytochrome *c* can be explained by a consideration of the individual contributions at each site of mutation. Arg38 likely contributes to the reduction potential of cytochrome *c* through two mechanisms, either via direct electrostatic stabilization of the reduced state of the heme group by the positively charged guanidinium side chain of this residue or through an electron-withdrawing

effect on the heme transmitted through the hydrogen-bonding network involving Wat121, Wat168, and the propionate A group of the heme (Figure 4; Cutler et al., 1989; Davies et al., 1993). The net result of these effects is a contribution of ~+45 mV to the reduction potential of the protein. The contribution of Asn52 to the reduction potential of cytochrome *c* likely has three elements. The first consists of the maintenance of hydrogen bonding about Wat166, an internal water molecule (Figure 5; Berghuis & Brayer, 1992; Berghuis et al., 1994a,b). Second is the dipole moment of the amide end of the side chain of Asn52, which is oriented to stabilize the reduced form of the heme iron (Langen et al., 1992). A third element is the hydrogen bond formed between the side chain of Asn52 and the propionate A group of the heme, which would be expected to have an electron-withdrawing effect on the heme. These three factors result in a contribution to the midpoint reduction potential of ~+55 mV.

Given that both Arg38 and Asn52 contribute to maintaining a high cytochrome *c* reduction potential through interaction with a common element, namely, the heme propionate A group, a strict additive calculation of the effect of the R38A and N52I mutations could overestimate the drop in reduction potential expected. As was shown experimentally (Table 10; Komar-Panicucci et al., 1992), this appears to be the case and suggests that in total, interactions with heme propionate A can only count toward raising the reduction potential of cytochrome *c* by some maximum value.

The mechanism by which substitution of Phe82 by serine affects reduction potential is different from that of either Arg38 or Asn52 substitution and is independent of residue replacements at these latter two positions. The predominant role of Phe82 appears to be in forming a part of the hydrophobic heme pocket and in excluding solvent from this pocket, and it contributes ~+40 mV to cytochrome *c* reduction potential through these mechanisms (Louie et al., 1988b; Lo et al., 1995). Phe82 does not appear to influence any structural features affected by either Arg38 or Asn52. This is supported by the observation that the reduction potentials of the R38A/F82S and N52I/F82S double-mutant proteins can be calculated simply by addition of the individual effects of each single-site substitution.

More difficult to analyze is the effect on reduction potential when all three substitutions are combined in one mutant protein. If it is assumed that all three mutations have independent and additive effects, the theoretical reduction potential (+147 mV) would be lower than the experimentally observed value (+162 mV; Table 10). As discussed previously, this discrepancy may be explained by the interdependence of the R38A and N52I mutations. However, addition of the effects of the R38A/N52I double mutant and the F82S mutant gives a theoretical reduction potential (+174 mV) which is greater than the observed experimental value (+162 mV). Therefore, the addition of the F82S mutation to the R38A/N52I double mutant has in some manner increased the net effect on the reduction potential of the protein. One possibility is that as multiple mutations are introduced, interactions between the three distal mutation sites are altered. Another possibility is that the cumulative alterations in side-chain packing resulting from the multiple mutations have functional consequences in addition to their structural effects. For example, it has been observed previously that the disruption of hydrophobic packing at a site which is distant from the heme group can affect the reduction potential of this latter group (Murphy et al., 1993). A third possibility arises from the fact that only one water molecule replaces the Arg38 side chain in the R38A/N52I/F82S mutant protein, whereas two water molecules are found in the other mutant proteins with the R38A substitution (Table 6). The presence of only one hydrogen-bonding group in this region of the protein may account for the discrepancy between the theoretical and observed reduction potentials. Evidence for this arises from consideration of the R38K mutant of yeast iso-1 cytochrome *c*, in which a drop in reduction potential of 23 mV is observed (Cutler et al., 1989). In this case, the substitution of Arg38 by lysine results in a decrease of available hydrogen-bonding groups while the positive charge of the side chain is maintained.

## CONCLUSIONS

Multiple mutations introduced within a single protein clearly affect functional and structural properties in different ways. In some cases the effects of multiple mutations are strictly additive, such as global protein stability in the present work, while the effects on other properties will be synergistic or partly so. This of course arises because within a single protein it is not uncommon that individual residues perform multiple functions and that these functions overlap with those of other residues. This poses a dilemma in understanding the roles of residues in protein function, especially in sorting out the individual contributions of each residue to each property. It also suggests that attempts at protein engineering, whether in modification of existing proteins or in attempts to develop new activities *de novo*, will be fraught with difficulties in assessing and compensating for the multiple roles of individual amino acids.

## ACKNOWLEDGMENT

The authors thank Yaoguang Luo for assistance with data collection, Nham Nguyen and Yili Wang for assistance in the crystallization of the cytochrome *c* mutant proteins, and Linda Comfort for assistance in the preparation of cytochrome *c* protein samples.

## REFERENCES

Berghuis, A. M., & Brayer, G. D. (1992) *J. Mol. Biol. 223*, 959–976.

Berghuis, A. M., Guillemette, J. G., McLendon, G., Sherman, F., Smith, M., & Brayer, G. D. (1994a) *J. Mol. Biol. 236*, 786–799.

Berghuis, A. M., Guillemette, J. G., Smith, M., & Brayer, G. D. (1994b) *J. Mol. Biol. 235*, 1326–1341.

Bushnell, G. W., Louie, G. V., & Brayer, G. D. (1990) *J. Mol. Biol. 214*, 585–595.

Connolly, M. L. (1983) *Science 221*, 709–713.

Cruickshank, D. W. J. (1949) *Acta Crystallogr. 2*, 65–82.

Cruickshank, D. W. J. (1954) *Acta Crystallogr. 7*, 519.

Cutler, R. L., Davies, A. M., Creighton, S., Warshel, A., Moore, G. R., Smith, M., & Mauk, A. G. (1989) *Biochemistry 28*, 3188–3197.

Das, G., Hickey, D. R., McLendon, D., McLendon, G., & Sherman, F. (1989) *Proc. Natl. Acad. Sci. U.S.A. 86*, 496–499.

Davies, A. M., Guillemette, J. G., Smith, M., Greenwood, C., Thurgood, A. G. P., Mauk, A. G., & Moore, G. R. (1993) *Biochemistry 32*, 5431–5435.

Guillemette, J. G., Barker, P. D., Eltis, L. D., Lo, T. P., Smith, M., Brayer, G. D., & Mauk, A. G. (1994) *Biochimie 76*, 592–604.

Hendrickson, W. A. (1985) *Methods Enzymol. 115*, 252–270.

Hickey, D. R., Berghuis, A. M., Lafond, G., Jaeger, J. A., Cardillo, T. S., McLendon, D., Das, G., Sherman, F., Brayer, G. D., & McLendon, G. (1991) *J. Biol. Chem. 266*, 11686−11694.
Higashi, T. (1990) *J. Appl. Crystallogr. 23*, 253−257.
Hildebrandt, P., Pielak, G. J., & Williams, R. J. P. (1991) *Eur. J. Biochem. 201*, 211−216.
Komar-Panicucci, S., Bixler, J., Bakker, G., Sherman, F., & McLendon, G. (1992) *J. Am. Chem. Soc. 114*, 5443−5445.
Langen, R., Brayer, G. D., Berghuis, A. M., McLendon, G., Sherman, F., & Warshel, A. (1992) *J. Mol. Biol. 224*, 589−600.
Leung, C. J., Nall, B. T., & Brayer, G. D. (1989) *J. Mol. Biol. 206*, 783−785.
Lo, T. P., Guillemette, J. G., Louie, G. V., Smith, M., & Brayer, G. D. (1995) *Biochemistry 34*, 163−171.
Louie, G. V., & Brayer, G. D. (1989) *J. Mol. Biol. 210*, 313−322.
Louie, G. V., & Brayer, G. D. (1990) *J. Mol. Biol. 214*, 527−555.
Louie, G. V., Hutcheon, W. L. B., & Brayer, G. D. (1988a) *J. Mol. Biol. 199*, 295−314.
Louie, G. V., Pielak, G. J., Smith, M., & Brayer, G. D. (1988b) *Biochemistry 27*, 7870−7876.
Luzzati, V. (1952) *Acta Crystallogr. 5*, 802−810.
Matthews, B. W. (1993) *Annu. Rev. Biochem. 62*, 139−160.
Mildvan, A. S., Weber, D. J., & Kuliopulos, A. (1992) *Arch. Biochem. Biophys. 294*, 327−340.
Moore, G. R., & Pettigrew, G. W. (1990) *Cytochromes c: Evolutionary, Structural and Physicochemical Aspects*, Springer-Verlag, Berlin.
Murphy, M. E. P., Fetrow, J. S., Burton, R. S., & Brayer, G. D. (1993) *Protein Sci. 2*, 1429−1440.
Rafferty, S. P., Pearce, L. L., Barker, P. D., Guillemette, J. G., Kay, C. M., Smith, M., & Mauk, A. G. (1990) *Biochemistry 29*, 9365−9369.
Sato, M., Yamamoto, M., Imada, K., Katsube, Y., Tanaka, N., & Higashi, T. (1992) *J. Appl. Crystallogr. 25*, 348−357.
Sherwood, C., & Brayer, G. D. (1985) *J. Mol. Biol. 185*, 209−210.
Tong, H., Berghuis, A. M., Chen, J., Luo, Y., Guss, J. M., Freeman, H. C., & Brayer, G. D. (1994) *J. Appl. Crystallogr. 27*, 421−426.
Wells, J. A. (1990) *Biochemistry 29*, 8509−8517.
Wilson, A. J. C. (1942) *Nature (London) 150*, 151−152.

BI942286O